Environmental Toxicology and Pharmacology 107 (2024) 104413

Contents lists available at ScienceDirect

Environmental Toxicology and Pharmacology

journal homepage: www.elsevier.com/locate/etap

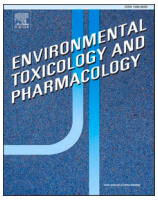

Physicochemical properties of 26 carbon nanotubes as predictors for pulmonary inflammation and acute phase response in mice following intratracheal lung exposure

Pernille Høgh Danielsen [a], Sarah Søs Poulsen [a], Kristina Bram Knudsen [a], Per Axel Clausen [a], Keld Alstrup Jensen [a], Håkan Wallin [b,c], Ulla Vogel [a,d,*]

[a] National Research Centre for the Working Environment (NFA), 105 Lersø Parkallé, Copenhagen Ø, Denmark
[b] National Institute of Occupational Health, Pb 5330 Majorstuen, Oslo 0304, Norway
[c] Department of Public Health, Section of Environmental Health, University of Copenhagen, Øster Farimagsgade 5A, Copenhagen K DK-1014, Denmark
[d] DTU Food, Technical University of Denmark (DTU), Anker Engelunds Vej 1, Lyngby DK-2800 Kgs, Denmark

ARTICLE INFO

Edited by Dr. M.D. Coleman

Keywords:
Carbon nanotubes
Inflammation
Acute phase response
Nanomaterial
Metals
Toxicity

ABSTRACT

Carbon nanotubes (CNTs) vary in physicochemical properties which makes risk assessment challenging. Mice were pulmonary exposed to 26 well-characterized CNTs using the same experimental design and followed for one day, 28 days or 3 months. This resulted in a unique dataset, which was used to identify physicochemical predictors of pulmonary inflammation and systemic acute phase response. MWCNT diameter and SWCNT specific surface area were predictive of lower and higher neutrophil influx, respectively. Manganese and iron were shown to be predictive of higher neutrophil influx at day 1 post-exposure, whereas nickel content interestingly was predictive of lower neutrophil influx at all three time points and of lowered acute phase response at day 1 and 3 months post-exposure. It was not possible to separate effects of properties such as specific surface area and length in the multiple regression analyses due to co-variation.

1. Introduction

Carbon nanotubes (CNTs) are hollow fiber-like nanomaterials that vary in physicochemical characteristics, such as, high aspect ratio, length, metal content, straightness, and surface functionalization. Single-walled carbon nanotubes (SWCNTs) consist of a single cylindrical carbon sheet layer whereas multi-walled carbon nanotubes (MWCNTs) consist of multiple layers of carbon sheets. Because of their unique structural properties, CNTs can be used in many industrial, commercial, and medical applications (De Volder et al., 2013; Jensen et al., 2015). Adverse responses, such as chronic inflammation, atherosclerosis, fibrosis and cancer are observed in different experimental systems exposed to CNTs, raising concerns about their health risk in human populations (Dong and Ma, 2019; Halappanavar et al., 2020; Kasai et al., 2015, 2016; Ma-Hock et al., 2009; Pauluhn et al., 2010), but especially workers can be exposed for more prolonged periods of time as compared to the general population (Canu et al., 2020). The International Agency for Research on Cancer Working Group evaluated the carcinogenicity of CNTs in 2014 and classified one specific type of MWCNT (MWCNT-7) as a group 2B carcinogen, whereas other types of MWCNTs and SWCNTs were not classifiable due to lack of experimental data (IARC, 2017). However, double walled carbon nanotubes and other types of MWCNTs have been shown to cause lung adenomas and mesotheliomas in two-year studies in rats (Rittinghausen et al., 2014; Saleh et al., 2022; Saleh et al., 2021). In the past, attention has particularly been drawn to the thin fiber-like structure and biopersistency of CNTs, suggesting that they may have toxicological effects similar to that of asbestos. Recently, the risk assessment committee (RAC) of the European Chemical Agency (ECHA) has adopted a proposal classifying MWCNT as category 1B carcinogens if their dimensions correspond to a geometric tube diameter range $\geq$ 30 nm to $<$ 3 μm and a length $\geq$ 5 μm and aspect ratio $\geq$ 3:1 (RAC, 2022). However, risk assessment for CNTs is generally challenging because of the large number of physicochemical properties that may vary between CNTs and that may influence toxicity (Bergamaschi et al., 2021). Grouping approaches have previously been successfully used to predict carcinogenic properties of long, thick and straight carbon nanotubes (Murphy et al., 2021, 2022) and to predict histopathological changes in lung (Fraser et al., 2021). Another approach to identify

* Corresponding author at: National Research Centre for the Working Environment (NFA), 105 Lersø Parkallé, Copenhagen Ø, Denmark.
E-mail address: ubv@nfa.dk (U. Vogel).

https://doi.org/10.1016/j.etap.2024.104413
Received 7 December 2023; Received in revised form 5 March 2024; Accepted 11 March 2024
Available online 13 March 2024

drivers of toxicity is to search for correlations between physicochemical properties and different outcomes. Using this approach, the specific surface area (BET) was identified as a positive predictor of pulmonary inflammation in multiple regression analyses in mice exposed to a panel of 10 different MWCNTs (Poulsen et al., 2016). CNT-induced inflammation and acute phase response are consistently observed in mice following pulmonary exposure (Knudsen et al., 2019; Labib et al., 2016; Nikota et al., 2016; Poulsen et al., 2015a,b, 2016, 2017; Poulsen et al., 2013; Rahman et al., 2017). Inflammation and acute phase response are early key events in adverse outcome pathways linking inhalation of various engineered nanomaterials including CNTs to cancer, fibrosis and atherosclerosis in Adverse Outcome Pathways (Halappanavar et al., 2020, 2023; Nikota et al., 2017; Nymark et al., 2021).

The objective of the present study was identify physico-chemical predictors of CNT-induced toxicity. We hypothesized, that physicochemical properties of the carbon nanotubes are predictive of the CNT-induced inflammation and acute phase responses. This end, we compiled data on pulmonary toxicity assessed in female mice exposed to a single dose of 26 different CNTs with different physicochemical properties and followed for 1, 28 days or 3 months using the exact same experimental design (Poulsen et al., 2016; Poulsen et al., 2013; Poulsen et al., 2015a; Solorio-Rodriguez et al., 2023). The majority of the CNTs are from two studies (Poulsen et al., 2016; Solorio-Rodriguez et al., 2023), which were designed to assess the effects of variation in diameter, length, and surface hydroxylation on CNT toxicity. In addition, we included widely studied MWCNTs from the JRC repository and MWNT-7, as the only CNT that is classified as possibly carcinogenic by IARC. The unique dataset of 26 CNTs was used to identify predictors between physicochemical properties (BET surface area, diameter, length, hydroxylation level, and metal content) and pulmonary inflammation (neutrophil influx) and systemic acute phase response (serum amyloid A3 (SAA3) plasma protein) using multiple regression analyses.

2. Methods

2.1. Nanomaterials and characterization

A total of seven SWCNTs and nineteen MWCNTs were included in the study. The SWCNTs (NRCWE-051 - NRCWE-057) and four of the MWCNTs (NRCWE-061 - NRCWE-064) were obtained from Timesnano (Chengdu Organic Chemicals Co. Ltd., China). Three MWCNTs (NM-401, NM-402 and NM-403) were obtained from the nanomaterial repository at the European Joint Research Centre, Ispra, Italy. Ten MWCNTs (NRCWE-040 – NRCWE-049) were obtained from Cheaptubes (Battleboro, VT, USA), NRCWE-026 was obtained from Nanocyl (Sambreville, Belgium) and NRCWE-006 (MWCNT-XNRI-7) was provided as a gift from Mitsui, Tokyo, Japan. The CNTs were pristine or surface-modified by the manufacturer, and they were not further modified before use.

The CNTs vary in the physicochemical properties, which are shown in Table 1 and supplementary tables S1-S3. The amount of OH given in Table 1 is based on the assumption that all oxygen measured in the CNTs by the combustion elemental analysis is in OH-groups.

The CNTs were investigated with wavelength dispersive X-ray fluorescence (XRF) in order to analyze the impurities of various elements within the respective samples. Approx. 0.5 g of each sample was weighed into a 40 mm-XRF-sample cup with Mylar 0.3 μm foil (Fluxana, Germany). Cotton were gently placed on the top of the powder, to hold it in place, and a sample lid was closing the cup. The prepared samples were analyzed using a Bruker Tiger S8 with a scan over all elements from Na to U with appropriate tube conditions (60 kV/67 mA; 50 kV/81 mA; 30 kV/135 mA). Measurements were automatically corrected for contribution from the foil, cotton and sampling cup. Analysis of all samples were in triplicate. All results are shown in Supplemental Materials Table S2. The results on the five metals, which are included in the multiple regression analyses are also given in Table 1.

The amount of nitrogen, hydrogen, carbon and oxygen in the samples (Supplemental Materials Table S1) were analyzed using combustion elemental analysis (CEA) performed by DB Lab A/S, Denmark, as previously described (Jackson et al., 2015).

The morphology of the CNTs was investigated via the computerized analysis of scanning electron microscopy (SEM) images. The diameters of the CNTs were from Poulsen et al., (2017). For NRCWE-040–049, the max circle radius diameter was used, which is acquired by automated measurements. The lengths of the SWCNTs could not be determined because of their tangled morphology. The SWCNTs bundled so strongly that the individual diameters could not be determined, but SWCNTs are typically reported having minimum diameters between 0.7 and 1 nm (Jensen et al., 2015).

The specific surface area were determined by the Brunauer, Emmett and Teller method (BET) by Quantachrome GmbH & Co. KG (Odelzhausen, Germany) as previously described (Danielsen et al., 2020).

2.2. Instillation suspensions and characterization

The CNT stock suspensions were prepared as previously described (Poulsen et al., 2016) in a concentration of 3.24 mg/ml in Nanopure water with 2% mouse serum and probe sonicated on ice, for 16 min with 10% amplitude without pause, using a Branson Sonifier S-450D (Branson Ultrasonics Corp., Danbury, CT, USA) equipped with a disruptor horn (model number 101–147–037). The stock suspensions were diluted to obtain 54, 18 and 6 μg per 50 μl, respectively and further sonicated for 2 minutes. The vehicle of Nanopure water added 2% mouse serum was similarly sonicated. 50 μl is the instillation volume per mouse.

The average hydrodynamic particle size (Z_{ave}) of the CNTs in instillation suspensions were determined by Dynamic Light Scattering (DLS; Malvern Nano Zetasizer equipment mounted with a 633 nm red laser) as described previously (Saber et al., 2016). The Z_{ave} distributions were measured both right after use and 3 hours after sonication (only the highest concentration). Data were obtained from six repeated analyses of each CNT sample. The intensity-based Z_{ave} and polydispersity index (PdI) of the CNT suspensions is shown in the Supplemental Materials Table S3. As DLS provide hydrodynamic sizes corresponding to a model for spheres, the DLS results inform the level of CNT dispersion, but may not inform directly on the quantitative hydrodynamic sizes of the CNTs. Especially not if separated into fibrous materials.

2.3. Animal procedures

The study complied with the EC Directive 86/609/EEC on the use of animals for laboratory experiments and was approved by the Danish 'Animal Experiments Inspectorate' (permissions: 2006/561–1123, 2010/561–1779, 2012–15–2934–00223). Prior to the study, the experimental protocols were approved by the local Animal Ethics Council. Female C57BL/6jBomtac mice (Taconic Europe, Ejby, Denmark), 7 weeks of age, were randomly distributed to cages containing animals for CNT exposure (N=7 mice/group for BAL, plasma and tissue collection and N=6 mice/group for histology) or to cages containing vehicle controls (N=3 mice/group). The mice had access to food (Altromin 1324, Brogaarden, Denmark) and tap water ad libitum.

At 8 weeks of age, the mice were anaesthetized by inhalation of 4% isoflurane and exposed to 50 μl CNT or vehicle suspension by a single intratracheal instillation into the lungs. Doses were 6, 18 and 54 μg/mouse. The instillation procedure has been described in detail previously (Hadrup et al., 2017; Saber et al., 2012). The animal experiments were performed over several weeks and vehicle controls were included on each exposure day. Mice were killed 1 day, 28 days or 3 months post-exposure by intramuscular injection of a Zoletil forte/ Rompun/ Fentanyl anesthetic cocktail in combination with heart blood withdrawal.

Table 1
Physicochemcal properties of the CNTs.

Name	Source	Length (nm)#	Diameter (nm)	Type	Functionalization	Carbon (%)	BET (m^2/g)	OH (mmol/g)$	Fe content*	Co content*	Ni content*	Mg content*	Mn content*
SWCNT													
NRCWE-051	Timesnano	-	1	SWCNT	Pristine	90.2	442.6	1.13	1.63	1.08	0.06	0.041	-
NRCWE-052	Timesnano	-	1	SWCNT	Pristine	92.9	405.7	0.83	1.05	1.23	0.12	0.028	0.009
NRCWE-053	Timesnano	-	1	SWCNT	-OH	88.2	367.8	1.85	0.85	3.82	0.10	0.021	0.023
NRCWE-054	Times nano	-	1	SWCNT	-COOH	87.9	370.8	3.03	1.59	3.81	0.13	0.027	-
NRCWE-055	Timesnano	-	1	SWCNT	Pristine	91.9	453.1	1.55	4.39	1.33	0.04	0.029	0.027
NRCWE-056	Timesnano	-	1	SWCNT	-OH	89.6	356.7	2.76	1.26	3.65	0.10	0.040	0.026
NRCWE-057	Timesnano	-	1	SWCNT	-COOH	83.1	281.6	6.02	2.20	2.74	0.14	0.177	0.044
MWCNT													
NM 401	JRC	4048 (±2371)	67 (±24)	MWCNT	Pristine	98.0	18	0.03	0.05	-	-	0.015	-
NM-402	JRC	1372 (±836)	11 (±3)	MWCNT	Pristine	91.0	226	0.28	1.31	-	0.001	0.001	0.001
NM-403	JRC	443 (±222)	12 (±7)	MWCNT	Pristine	96.9	135	0.19	0.003	1.12	0.002	0.188	0.16
NRCWE-061	Timesnano	730.85	16.42	MWCNT	$-NH_2$	96.5	170.4	0.42	0.59	0.001	1.97	0.010	0.005
NRCWE-062	Timesnano	468	8.82	MWCNT	Pristine	89.1	443.2	2.59	0.58	4.60	0.22	0.074	-
NRCWE-063	Timesnano	345.35	14.18	MWCNT	-OH	88.2	426.4	2.66	1.95	5.87	0.49	0.072	0.023
NRCWE-064	Timesnano	213.6	7.46	MWCNT	-COOH	88.4	445.2	3.21	1.80	5.51	0.30	0.027	0.028
NRCWE-040	Cheaptubes	518.9 (±598)	22.1 (±7.8)	MWCNT	Pristine	95.5	150	0.35	0.20	0.001	0.56	0.01	0.002
NRCWE-041	Cheaptubes	1005 (±2948)	26.9 (±10.1	MWCNT	-OH	93.7	152	1.69	0.13	0.001	0.31	0.02	0.001
NRCWE-042	Cheaptubes	723.2 (±971.9)	30.2 (±14.2)	MWCNT	-COOH	99.2	141	4.09	0.08	0	0.21	0.03	0.001
NRCWE-043	Cheaptubes	771.3 (±3471)	55.6 (±18.1)	MWCNT	Pristine	96.0	82	0.18	0.008	0.001	1.2	0.01	-
NRCWE-044	Cheaptubes	1330 (±2454)	32.7 (±13.6)	MWCNT	-OH	96.1	74	0.23	0.004	0.002	1.04	0.02	-
NRCWE-045	Cheaptubes	1553 (±2954)	30.2 (±15.6)	MWCNT	-COOH	91.6	119	0.63	1.17	0.25	1.34	0.02	0.002
NRCWE-046	Cheaptubes	717.2 (±1214)	29.1 (±16.1)	MWCNT	Pristine	95.1	223	0.63	0.008	0.25	0.0045	0.22	0.3
NRCWE-047	Cheaptubes	532.5 (±591.9)	22.6 (±10.1)	MWCNT	-OH	96.1	216	0.26	0.007	0.25	0.0043	0.22	0.3
NRCWE-048	Cheaptubes	1604 (±5609)	17.9 (±17.9)	MWCNT	-COOH	95.3	185	0.58	0.007	0.24	0.0037	0.19	0.28
NRCWE-049	Cheaptubes	731.1 (±1473)	14.9 (±5.6)	MWCNT	$-NH_2$	96.0	199	0.33	0.004	0.25	0.0038	0.19	0.29
NRCWE-026	Nanocyl	847 (±446)	11 (±3)	MWCNT	Pristine	85.5	254	0.79	0.26	0.106	0.001	-	-
NRCWE-006	Mitsui/Hadogaya	5730 (±491)	74 (±29)	MWCNT	Pristine	98.1	26	0.08	0.08	-	-	0.013	-

The lengths were determined by computerized image analysis of SEM micrographs. $ The OH is the amount of functionality assuming that all oxygen measured by CEA was OH-groups. * Determined by XRF. Chemical composition data were calculated as wt% of all the oxides measured. Thorough characterization of all the CNTs has been published previously (Jackson et al., 2015, Poulsen et al., 2016, Knudsen et al., 2019 Solorio-Rodriguez et al., 2023). -: Not detected

2.4. BAL cells and tissue collection

In brief, BAL fluid was recovered by flushing the lungs twice with 1 ml saline in a syringe. Each flush was performed with fresh saline. The BAL fluid was stored on ice until separation of cells by centrifugation at 400 x *g* for 10 min at 4 °C. The separated BAL cells were re-suspended in 100 µl HAMF12 medium with 10% fetal bovine serum. The total number of viable cells and of dead cells was determined from 20 µl diluted cell suspension by NucleoCounter NC-200 (Chemometec, Allerød, Denmark). For differential counting of macrophages, neutrophils, lymphocytes and eosinophils, 40 µl of the fresh cell suspension was collected on microscope slides and centrifuged at 60 x *g* for 4 min. Then the cells were fixed with 96% ethanol and incubated with May-Grünwald-Giemsa stain. Differential counts were determined by counting 200 cells per sample under light microscope.

2.5. SAA3 protein level in plasma

Plasma levels of SAA3 protein were determined using ELISA in according to the manufacturer's protocol (Mouse Serum Amyloid A-3, Cat. # EZMSAA3–12 K, EMD Milipore) (Poulsen et al., 2017). For each dose group three mice were randomly selected. At day 1, all three dose levels were included. At day 28 and 90, only the highest dose (54 µg/mouse) was analyzed. Control groups included 23 mice in total (1 day post-exposure: n=11; 28 days post-exposure: n=5; 3 months post-exposure: n=7).

2.6. ANOVA for group comparisons

The data sets of BAL cells and plasma levels of SAA3 protein were analyzed using the software package Graph Pad Prism 8.1.2. (Graph Pad Software Inc., La Jolla, CA, USA). All data are expressed as mean ± standard deviation. For all analyses the vehicle controls were combined for each post-exposure time. Data were tested for normality using the Shapiro-Wilks test and for variance homogeneity using the Bartlett's test. The effects of exposure and dose were analyzed by ordinary one-way ANOVA on log-transformed data and corrected for multiple comparison using Dunnet's test. A P-value ≤ 0.05 was considered significant.

2.7. Pearson correlation

All physicochemical parameters, except BET surface area, were log-transformed using base 2. For BET surface area, we used log(BET)/log (1.25). OH- and COOH-functionalization was determined by the same combustion elemental analysis: Functionalization levels were calculated under the assumption that all oxygen atoms were either OH or COOH, respectively (Jackson et al., 2015). Oxygen content was therefore chosen as OH-functionalization in the statistical analyses. Aluminum was omitted due to a large number of missing values. All correlation analyses were performed in SAS version 9.4 (SAS Institute Inc., Cary, NC, USA).

The pairwise associations between physicochemical parameters (BET surface area, Fe, Mn, Ni, Co, Mg, diameter, length and functionalization) of the CNTs were investigated graphically in a Pearson Correlation analysis. In addition, we included a binary variable named "Multi", which is denoted "1" for MWCNTs and "0" for SWCNTs.

2.8. Multiple regression analyses

We included indicator variables for below detection limit to insure that the imputed values did not affect the estimated association between the outcome and the chemical composition. For the multiple logistic regression analyses, problematic zero-values were identified using 2×2 cross tables. If the relationship between variable and the outcomes relied completely on the zero-values, then this and the CNT type, was removed from the specific analysis. All multiple regression and multiple logistic regression analyses were performed in SAS version 9.4 (SAS Institute Inc., Cary, NC, USA). As many analyses were performed, there are a risk of mass-significance, however adjustments for mass significance effects was avoided by using a statistical significance level at 0.01 instead of 0.05 in the multiple regression and multiple logistics regression analyses.

3. Results

3.1. Physicochemical properties

The main physicochemical characteristics of the full CNT dataset used in the multiple regression analyses are summarized in Table 1. All other measured properties are shown in the Supplemental Materials (Table S1 and Table S2).

3.2. Cell composition in bronchoalveolar lavage fluid

Recruitment of inflammatory cells in BAL fluid was assessed 1 day, 28 days and 3 months post-exposure to a single dose of CNTs as a biomarker of the pulmonary inflammatory response. The distributions of total number of cells and the number of macrophages, neutrophils, eosinophils and lymphocytes were determined.

Dose-dependent neutrophil influx was observed at day 1 post-exposure for all the CNTs (Fig. 1). The number of neutrophils was markedly lower at day 28 post-exposure compared to day 1 post-exposure (Fig. 2). The increased number of neutrophils observed for some CNTs at day 28 post-exposure remained significantly increased at 3 months post-exposure at the highest dose level (Supplemental Materials Fig. S1).

The full dataset of the BAL cell composition is shown in the Supplemental Materials (Table S4a – S4f). In brief, these results show that the total number of cells in BAL fluid are significantly increased at day 1 post-exposure for most CNT types, but the increase remains only significant at day 28 and 3 months post-exposure for few of the CNTs (Supplemental Table S4a). For a few CNTs, pulmonary exposure results in lower levels of macrophages in BAL fluid at day 1 post-exposure, whereas at day 28 and 3 months post-exposure there are few CNTs causing significant increased levels of macrophages (Supplemental Table S4b). No increase in the number of lymphocytes at day 1 post-exposure was observed, whereas few CNTs increased the level of lymphocytes at day 28 and 30 months post-exposure (Supplemental Table S4c). The number of eosinophils was highly increased at day 1 post-exposure (Supplemental Table S4e), similarly to neutrophils (Supplemental Table S4d). The increased eosinophil levels was almost completely diminished at day 28 post-exposure for most CNTs (Supplemental Table S4e).

3.3. Acute phase response

The acute phase response was measured as SAA3 protein levels in plasma for all dose levels at day 1 post-exposure and for 54 µg at day 28 and 3 months post-exposure. Dose-dependency was observed for SAA3 protein levels at day 1 for all the CNTs. The level of SAA3 protein was statistically significantly increased 1 day post-exposure as compared to vehicle control for all CNTs, at either the two highest or the highest dose level except for NRCWE-040 and NRCWE-046 (Fig. 3A). The increase in SAA3 protein levels was diminished at day 28 and 3 months post-exposure as compared to day 1 post-exposure (Figs. 3B and 3C). Statistically significant correlations were observed between SAA3 protein in plasma and neutrophil influx at day 1 and day 28 post-exposure (Fig. 4). Neutrophil influx has a large dynamic range, and we therefore decided to use neutrophil influx as a biomarker of both inflammation and acute phase response, since we have consistently observed close correlation between nanomaterial-induced neutrophil influx, SAA3 levels in plasma and *Saa3* mRNA levels in lung tissue (Gutierrez et al., 2023; Hadrup et al., 2020; Poulsen et al., 2017; Saber et al., 2014).

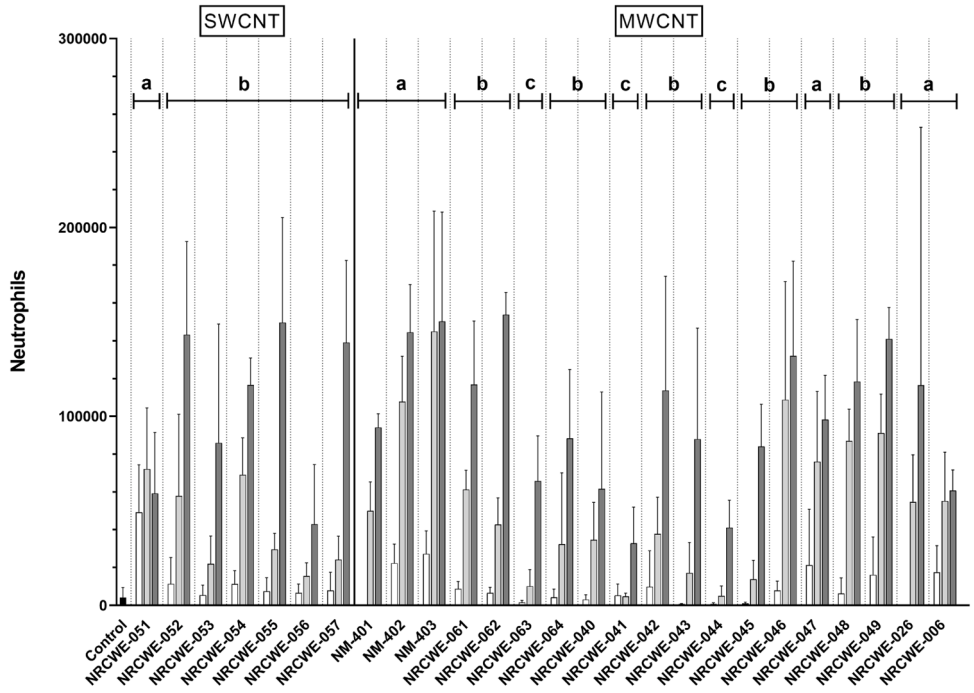

Fig. 1. The number of neutrophils in BAL fluid 1 day post-exposure. All values are presented as mean±SD. Control (black bar); 6 μg/ mouse (white bar); 18 μg/ mouse (light grey bar); 54 μg/ mouse (dark grey bar). Significantly increased compared to the control: **a**) all doses (6, 18 and 54 μg/mouse), **b**) the two highest doses (18 and 54 μg/mouse) and **c**) the highest dose (54 μg/ mouse).

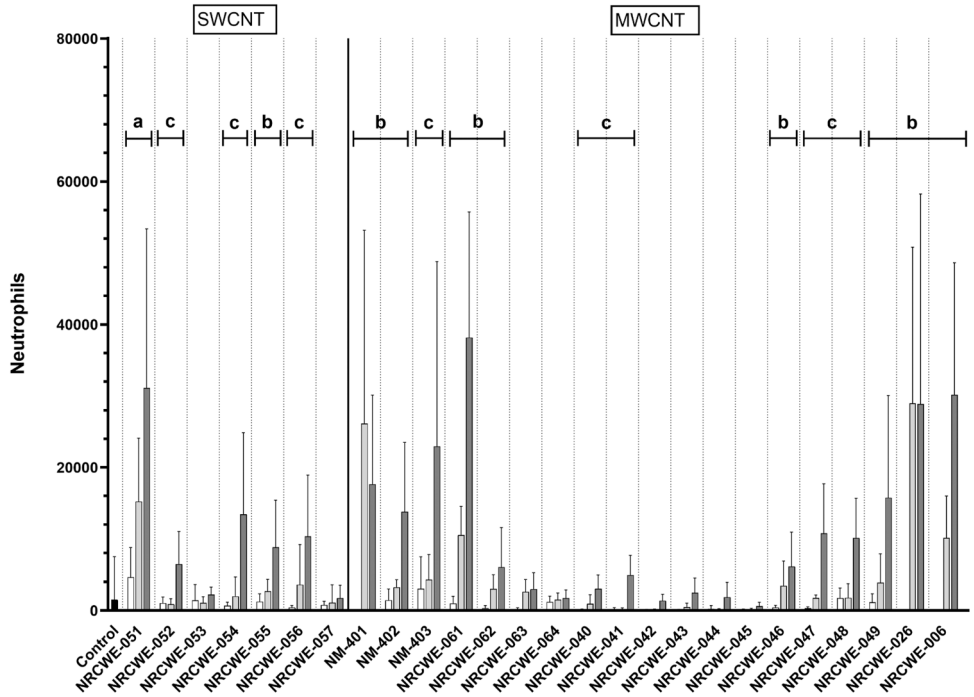

Fig. 2. The number of neutrophils in BAL fluid 28 days post-exposure. All values are presented as mean±SD. Control (black bar); 6 μg/ mouse (white bar); 18 μg/ mouse (light grey bar); 54 μg/ mouse (dark grey bar). Significantly increased compared to the control: **a**) all doses (6, 18 and 54 μg/mouse), **b**) the two highest doses (18 and 54 μg/mouse) and **c**) the highest dose (54 μg/ mouse).

3.4. Pearson correlation for identification of independent physicochemical properties

For neutrophil influx and SAA3 protein levels, the pairwise associations between physicochemical parameters (BET surface area, Fe, Mn, Ni, Co, Mg, diameter, length, and functionalization) of the CNTs were investigated in a Pearson Correlation analysis. In addition, we included a binary variable named "Multi", which is denoted "1" for MWCNTs and "0" for SWCNTs.

For neutrophil influx, clusters of highly correlated parameters were identified. Cluster 1: BET surface area, diameter, length, Co and 'Multi'. Cluster 2: Mn and Mg. The parameters in these clusters could not be

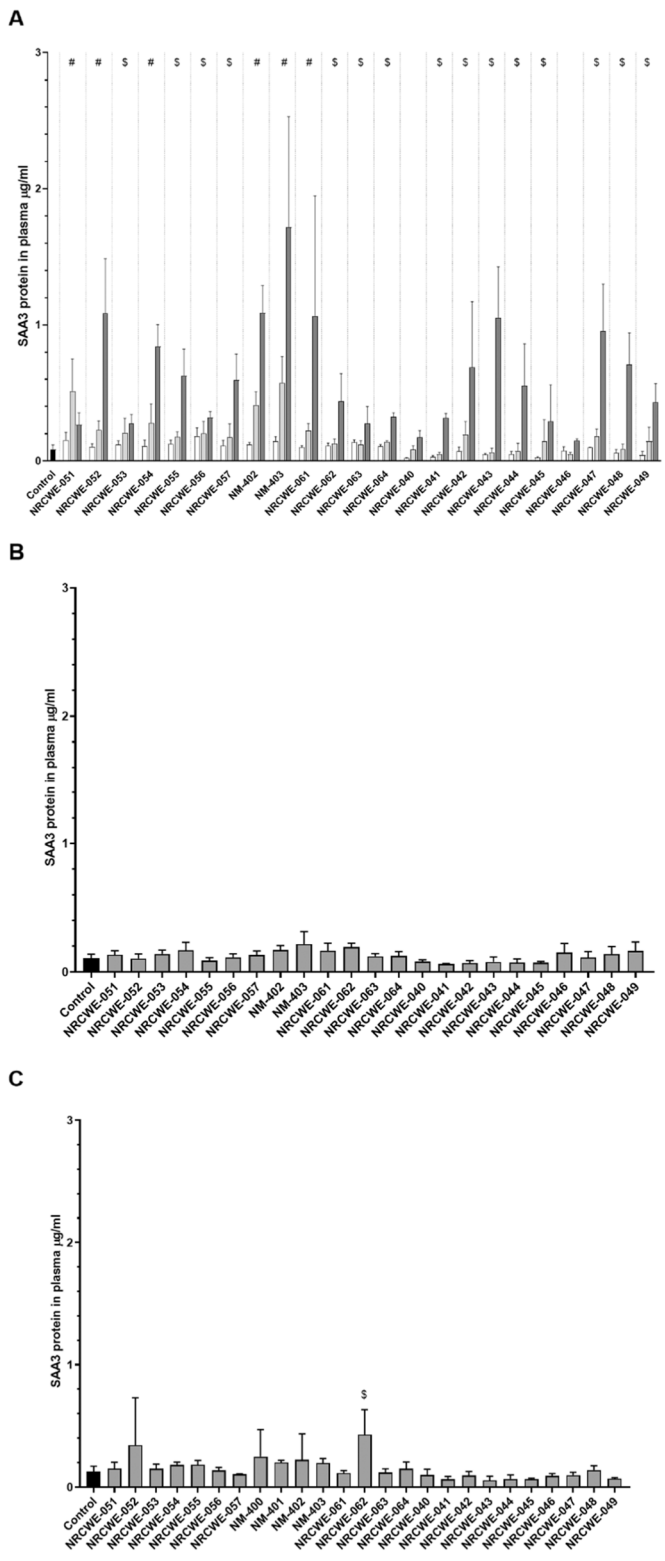

Fig. 3. SAA3 plasma protein levels at day 1 (A), day 28 (B) and 3 months (C) post-exposure. All values are presented as mean±SD. Individual particles marked with # show significantly increased SAA3 plasma protein levels compared to the control for the two highest dose levels, when marked with $ the significant increase compared to the control is only for the highest dose.

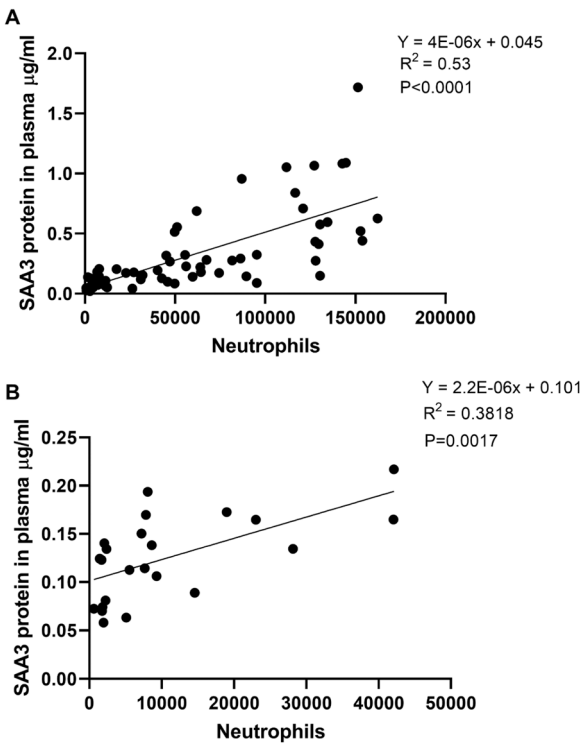

Fig. 4. Correlation plot for SAA3 plasma protein levels and neutrophil influx 1 day (A) and 28 days (B) post-exposure. Each dot represents the mean of three mice exposed to either 6, 18 or 54 µg of 22 CNTs.

separated. The Ni, Fe, and OH-functionalization variables were all independent (Supplemental Materials Table S5).

The large dataset (MWCNT/SWCNT, n=26) was also divided into SWCNTs or MWCNTs. New Pearson Correlation analyses were subsequently performed for each new dataset.

Pearson Correlation analysis for the MWCNTs only (n=19) revealed two clusters of highly correlated parameters. Cluster 1: BET surface area, diameter, length and Co and cluster 2: Mn and Mg. These parameters could not be separated. Ni, Fe, and OH-functionalization were independent variables (Supplemental Materials Table S6).

Pearson Correlation analysis for the SWCNTs only (n=7) revealed one cluster of highly correlated parameters: BET surface area and OH. These parameters could not be separated. Length was omitted, as it was not possible to measure it for the SWCNTs (Solorio-Rodriguez et al., 2023). Diameter was also omitted as all SWCNTs were set to a diameter of 1 nm. The remaining parameters (Fe, Mn, Ni, Co, and Mg) were independent variables (Supplemental Materials Table S7). The different clusters and independent variables are summarized in Table 2.

Similarly, for SAA3 protein, the pairwise associations between physicochemical parameters of 25 CNTs, 18 MWCNTs and 7 SWCNTs were investigated in a Pearson Correlation. SAA3 protein data were not available from NRCWE-006-exposed mice and therefore the particle type was omitted from the analysis revealing a slightly altered result. Overall, the same clusters were identified, as described above, except that OH now is included in cluster 1 for the analysis of all CNTs and for the analysis of MWCNTs only (Table 2). The detailed tables are shown in the Supplemental Materials Table S8, S9 and S10.

3.5. Multiple regression analyses

With the aim of identifying physicochemical properties of CNTs important for their toxicity, the effect of dose, BET surface area, metal and oxygen content on neutrophil influx and SAA3 plasma protein was analyzed by multiple regression (Tables 3 and 4).

Table 2
Pearson correlation analyses of physicochemical parameters across the analyzed CNT datasets.

Neutrophil influx		
CNTs	**Cluster**	**Individual**
MWCNT/SWCNT N=26	Cluster 1: Diameter, BET surface area, length, Co, Multi Cluster 2: Mn, Mg	Fe, Ni, OH
MWCNT N=19	Cluster 1: Diameter, BET surface area, length, Co Cluster 2: Mn, Mg	Fe, Ni, OH
SWCNT N=7	Cluster: BET, OH	Ni, Co, Fe, Mn, Mg
SAA3 plasma protein		
CNTs	**Cluster**	**Individual**
MWCNT/SWCNT N=25	Cluster 1: Diameter, BET surface area, length, Co, multi, OH Cluster 2: Mn, Mg	Fe, Ni
MWCNT N=18	Cluster 1: Diameter, BET surface area, length, Co, multi, OH Cluster 2: Mn, Mg	Fe, Ni
SWCNT N=7	Cluster: BET, OH	Ni, Co, Fe, Mn, Mg

Table 3
Multiple regression analyses of CNT physicochemical properties as predictors of neutrophil influx.

	Exposure variable (per doubling)	Day 1	Day 28	3 months
MWCNT/SWCNT	Dose	**1.054 (<.0001)**	**1.068 (<.0001)**	ND
	[a] **Multi**	1.301 (0.1991)	1.648 (0.1415)	**0.127 (0.0003)**
	Ni	**0.834 (<.0001)**	**0.788 (<0.001)**	**0.628 (<.0001)**
	[b] **Mn**	**1.125 (0.0006)**	**1.446 (<.0001)**	**1.113 (0.2433)**
	Fe	**1.114 (0.0005)**	**1.450 (<.0001)**	1.015 (0.8635)
	OH	0.915 (0.1793)	**0.591 (<.0001)**	0.847 (0.3681)
MWCNT	Dose	**1.055 (<.0001)**	**1.074 (<.0001)**	ND
	[c] **Diameter**	**0.584 (0.0097)**	**0.277 (0.0003)**	0.669 (0.5642)
	Ni	**0.872 (<.0001)**	**0.868 (0.0074)**	**0.644 (<.0001)**
	[b] **Mn**	1.020 (0.6521)	1.202 (0.0159)	1.061 (0.6832)
	Fe	0.997 (0.9558)	1.111 (0.2077)	0.954 (0.7709)
	OH	0.935 (0.3341)	0.739 (0.0181)	0.869 (0.5663)
SWCNT	Dose	**1.052 (<.0001)**	**1.056 (<.0001)**	ND
	[d] **BET**	0.912 (0.7936)	**3.591 (0.0120)**	**2.099 (0.0114)**
	Ni	0.819 (0.6145)	0.723 0.5716)	0.919 (0.7929)
	Co	0.788 (0.3036)	0.788 (0.4759)	1.270 (0.2044)
	Mn	[e] ND	[e] ND	[e] ND
	Mg	[e] ND	[e] ND	[e] ND
	Fe	[e] ND	[e] ND	[e] ND
	OH	-	-	-

Values are the Multiplicative Effect and p-values are shown in brackets. Significant p-values ($P<0.01$) are highlighted in bold. ND: not determined.
[a] **Multi**: proxy variable for the highly correlated diameter, length, BET, and Co content.
[b] **Mn**: proxy variable for the highly correlated Mg content.
[c] **Diameter**: proxy variable for the highly correlated length, BET and Co content.
[d] **BET (per 25% difference instead of per** doubling**)**: proxy variable for the highly correlated OH content.
[e] Omitted due to lack of individual effect on the outcome.

In the first approach, all CNTs (MWCNT/SWCNT) were analyzed in one dataset as predictors of neutrophil influx. Based on the Pearson correlation analysis, 'multi' was chosen as proxy variable for cluster 1 and Mn was chosen as proxy variable for cluster 2, as these variables displayed good tolerance and explained most of the variance as compared to the other variables in the clusters.

In a second analysis, MWCNT and SWCNT were analyzed separately in order to study the physicochemical predictors for the two CNT classes. For each analysis, the most significant predictors were identified and the best proxy/most significant proxy for each group was used. Thus, different proxies were used in the three analyses.

For the MWCNT dataset, diameter was chosen as proxy variable for cluster 1, whereas Mn was chosen as proxy variable for cluster 2. For the SWCNT dataset, BET surface area was chosen as the best proxy variable for the identified cluster. Due to the limited number of data points for the SWCNT only dataset, we were forced to omit the variables that did not show individual association with the endpoints from the regression analyses.

The analysis of neutrophil influx showed that dose was significantly predictive on day 1 and 28 after exposure for SWCNT alone, MWCNT alone and for MWCNT/SWCNT. The content of Ni was significantly predictive of lower neutrophil influx in lung BAL fluid on day 1, 28 and 3 months after exposure (MWCNT, MWCNT/SWCNT). The content of Mn and Fe significantly predicted a higher neutrophil influx on day 1 and 28 after exposure (MWCNT/SWCNT). The content of OH predicted a lower neutrophil influx at day 28 after exposure (MWCNT/SWCNT). Diameter was significantly predictive of lower neutrophil influx on day 1 and 28 after exposure (MWCNT). An effect of being multi-walled or single-walled was identified, and showed that SWCNTs were more inflammogenic in terms of neutrophil influx as compared to MWCNTs 3 months after exposure.

A similar approach was done for SAA3 plasma protein levels. For the

Table 4
Multiple regression analyses of CNT physicochemical properties as predictors of SAA3 plasma protein.

	Exposure variable (per doubling)	Day 1	Day 28	3 months
MWCNT/SWCNT	Dose	**1.037 (<.0001)**	ND	ND
	[a] **BET**	1.070 (0.0882)	1.018 (0.6532)	0.076 (0.0503)
	[b] **Mn**	0.979 (0.4649)	1.040 (0.1875)	0.969 (0.3128)
	Ni	**0.914 (<.0001)**	0.959 (0.0444)	**0.931 (0.0002)**
	Fe	1.016 (0.5386)	1.021 (0.4239)	1.033 (0.2370)
MWCNT	Dose	**1.042 (<.0001)**	ND	ND
	[c] **Diameter**	**0.584 (0.0002)**	0.756 (0.0364)	0.666 (0.0215)
	[b] **Mn**	0.945 (0.0477)	1.043 (0.1223)	1.029 (0.4024)
	Ni	0.951 (0.0378)	0.962 (0.086)	0.974 (0.2778)
	Fe	0.947 (0.0702)	1.022 (0.4386)	1.033 (0.3696)

Values are the Multiplicative Effect and p-values are shown in brackets. Significant p-values ($P<0.01$) are highlighted in bold. ND: not determined.
[a] BET (per 25% difference instead of per doubling): proxy variable for the highly correlated Multi variable, diameter, length, Co and OH content.
[b] Mn: proxy variable for the highly correlated Mg content.
[c] Diameter: proxy variable for the highly correlated length, BET surface area, Co and OH content.

dataset on MWCNT/SWCNT, BET surface area was chosen as proxy variable for cluster 1 and Mn was chosen as proxy variable for cluster 2. For the MWCNT dataset, diameter was chosen as proxy variable for cluster 1, whereas Mn was chosen as proxy variable for cluster 2. Due to the limited number of data points for the SWCNT dataset and lack of individual effect on the outcome the multiple regression analyses for this dataset was not performed.

The analysis showed that dose was significantly predictive of higher SAA3 plasma protein levels on day 1 after exposure for MWCNT/SWCNT and MWCNT alone. At day 28 and 3 month, only the highest dose was analyzed, so dose was not a variable. The Ni content was significantly predictive for lower levels of SAA3 plasma protein on day 1 and 3 months after exposure (MWCNT/SWCNT). Diameter was significantly predictive of lower levels of neutrophil influx on day 1 after exposure (MWCNT).

4. Discussion

In the present study, we investigated pulmonary toxicity of CNTs in terms of inflammation (influx of neutrophils into the lung) and systemic acute phase response (SAA3 plasma protein).

Inflammation has been identified as an important key event following pulmonary exposure to particles linked to several adverse outcomes including cancer, fibrosis and chronic obstructive pulmonary disease (COPD) (Halappanavar et al., 2021a, 2021b, 2020). It has previously been demonstrated that CNT-induced neutrophil influx is accompanied by increased pulmonary expression of inflammation-related genes both at RNA and protein levels (Bornholdt et al., 2017; Labib et al., 2016; Nikota et al., 2017; Rahman et al., 2017; Serra et al., 2022; Solorio-Rodriguez et al., 2023). We use neutrophil influx in BAL fluid as a robust and sensitive biomarker of an inflammatory response.

Induction of acute phase response is causally related to increased risk of cardiovascular disease (Gabay and Kushner, 1999; Hadrup et al., 2020; King et al., 2011; Saber et al., 2014). Specifically, the acute phase response protein serum amyloid A is causally implicated in atherosclerosis (Thompson et al., 2018). Mice and humans have similar acute phase response system, and both express SAA. Thus, overexpression or pulmonary exposure to SAA promotes plaque progression in susceptible mouse models (Christophersen et al., 2021; Dong et al., 2011; Thompson et al., 2018). We have previously reported induction of acute phase response following pulmonary exposure to very different CNTs that induced strong pulmonary and hepatic acute phase responses accompanied by changes in the lipid profiles (Poulsen et al., 2015b, 2017). We focused on systemic acute phase response, in terms of SAA3 protein levels in plasma, in the present animal studies, as this is the biomarker that is readily available in humans. In the current study, CNT-exposure increased SAA3 levels from 0.1 mg/L to 1–2 mg/L, i.e. 10–20 fold. This is comparable to the ca. 20-fold dose-dependent increase in SAA levels in blood observed in a controlled human study, where healthy volunteers were exposed to 0, 0.5, 1 and 2 mg/m^3 ZnO nanoparticles for 4 hours on separate occasions (Monsé et al. 2018).

In this study, we used intratracheal instillation, which is suitable for hazard comparison, because it allows full control of the deposited dose, even though inhalation is the gold standard for risk assessment of airborne materials. For the current analysis, it is essential that the CNT dose is well determined, whereas the deposited dose can vary considerably for aerosolized CNTs (Gate et al., 2019). We have previously demonstrated that intratracheal instillation of CNTs results in an even distribution across most long lobes (Poulsen et al., 2016). Additionally, good correspondence was observed between CNT-induced neutrophil influx between inhalation and instillation exposure (Cosnier et al., 2021). As described in a previous study (Poulsen et al., 2016), the dose levels correspond to a third, 1 or 3 times the expected 40-year exposure for workers at the recommended exposure limit of 1 μg carbon/m^3 (NIOSH, 2013), when assuming 10% deposition (Ma-Hock et al., 2009), a ventilation rate of 1.8 l/h for mice, and a 40 h working week. The time points were chosen to reflect acute (post-exposure day 1), sub-acute (post-exposure day 28) and sub-chronic (post-exposure day 90) post-exposure time points that would enable comparison with inhalation studies such as the study by Pauluhn, (2010), who included these post-exposure time points.

All the studied CNTs induce dose-dependent inflammation in terms of neutrophil influx day 1 after exposure. The neutrophil influx decreased at day 28 and 3 months post-exposure as compared to day 1. All the CNTs showed dose-dependently increased SAA3 protein levels in plasma at day 1 after exposure. Furthermore, SAA3 plasma levels correlated closely with neutrophil influx across CNT types and post-exposure time points. We have previously observed similar close correlations across soluble and insoluble metal oxide particles (Gutierrez et al., 2023) and observed the same close correlations with *Saa3* mRNA levels in lung tissue across inhalation and instillation exposure, post-exposure time points and types of nanomaterials (Bengtson et al., 2017; Danielsen et al., 2020; Di Ianni et al., 2020; Hadrup et al., 2019; Poulsen et al., 2017; Saber et al., 2013). The present results suggests that SAA blood levels and neutrophil influx can be used as proxies for each other.

In the multiple regression analysis of SWCNT, dose (day 1 and day 28 post-exposure) and BET (day 28 and 3 months post-exposure) were positive predictors of neutrophil influx. For MWCNTs, MWCNT diameter was the best proxy for the cluster of variables diameter, length, BET surface area and Co content. Diameter was associated with lower inflammatory response at 1 and 28 days post-exposure in agreement with our previous assessment of 10 MWCNT (Poulsen et al., 2016) and

Cosnier et al., who reported that the surface area dose of CNTs retained within the lung predicted neutrophil influx in inhalation studies in rats (Cosnier et al., 2021). The present Ni concentrations was also predictive of lower inflammatory response at all three time points.

When all MWCNTs and SWCNTs were included in the same multiple regression analysis, the classifier 'Multi', which distinguishes between MWCNTs and SWCNTs, was predictive of lower inflammation at 3 months but not predictive at day 1 and 28. In agreement with this, we recently reported that the SWCNTs NRCWE-051–057 and MWCNTs NRCWE-060–64 in the present study had very similar global pulmonary transcriptional signatures at day 1 post-exposure (Solorio-Rodriguez et al., 2023). Again, the Ni content was predictive of a lower inflammatory response at all post-exposure time points as also seen for MWCNTs alone, whereas Fe and Mn (Mn proxy for both Mn and Mg) were predictive of increased inflammation at day 1 and 28 after exposure. Fe-oxides are known to induce lung inflammation in mice after intratracheal instillation (Hadrup et al., 2020) but we aslo note that in the combined analysis of SWCNTs and MWCNTs, Fe was negatively correlated with diameter (correlation coefficient −0.61, Table S5). Thus, it is possible that the observed correlations between Fe content and inflammation is driven by this association. Despite the important role in a number of physiological processes, Mn has been implicated in inducing pulmonary toxicity even though little is known about the potential pulmonary effects and the underlying molecular mechanisms (Gandhi et al., 2022). A nose-only inhalation study in mice exposed to 2 mg Mn(II)/m^3 for 5 days showed no significant pulmonary inflammation but induced altered pulmonary gene expression in pathways related to susceptibility to respiratory diseases such as asthma and COPD (Bredow et al., 2007). A study showed increased pulmonary toxicity (tissue damage markers and histology) in rats exposed via intratracheal instillation to MgO at a dose of 1 mg/kg or 5 mg/kg into lungs at 1, 7, and 30 days of post-exposure (Gelli et al., 2015). The concentrations of Fe, Mn and Mg (trace elements) identified in the present study are much lower than the mentioned exposure doses of metal oxides. However, the metal contents are up to 5–6 wt% for some CNTs, which amounts to 3 μg at the highest dose level. In a previous study, we have assessed combination effects of surface area and Cu-content using metal-doped amorphous silica particles (Hadrup et al., 2021). The Cu doses were in the range of 0.5–4.7 μg/animal and induced neutrophil influx at 1.4 and 4.7 μg/mouse. In general, the analyses of the metal contents suffer from the fact that metal types and contents vary considerably between the studied CNTs, and thus, we were not able to include all the metals in the analysis (Supplementary tables S1-S2).

For SAA3 plasma protein levels, multiple regression analyses of SWCNTs alone were not performed, since only the dose was predictive of SAA3 levels. For the MWCNTs, diameter was predictive of lower inflammatory response 1 day post-exposure, similar to neutrophil influx. In the combined analysis of SWCNT and MWCNT, the classifier 'multi' was not predictive of SAA3 levels (BET surface area as proxy variable), suggesting that MWCNT and SWCNT have similar effects on CNT-induced acute phase response.

Interestingly, Ni content was associated with lowered acute phase response at day 1 and 3 months, similar to the analysis of neutrophil influx. In the previous analysis of 10 of the MWCNTs the apparent protective effect of Ni on inflammation was suggested to be driven by the covariance with other physicochemical properties [8]. However, in the present multiple regression analyses Ni is considered an individual variable. Ni is a potent inducer of respiratory allergic responses (Roach et al., 2019). We speculated whether it is possible that such an allergic response (i.e. induction of eosinophils) would reduce inflammatory and acute phase responses. A study have shown that instillation of gradually dissolving NiO NPs in rats produced massive eosinophilic inflammation during the period of acute neutrophilic inflammation, but with a delayed time-frame at 3 and 4 days post-exposure (Lee et al., 2016). We do not have data for day 3 post-exposure for all the CNTs and cannot investigate the early time course in the present study. However, we find that the number of neutrophils and eosinophil correlate at day 1 and that the number of eosinophils are not correlated to the concentrations of Ni in the present study (data not shown). The biological mechanism-of-action underlying Ni-associated lowering of the inflammatory response and the acute response therefore remains unclear. In future analysis, it is necessary to further identify the speciation and dissolution behavior of identified metals to unravel their potential mechanisms of action.

The linear regression analyses with SAA3 suffered from limited statistical power at days 28 and 3 months post-exposure, as only the high dose level was included on these post-exposure time points. In addition, the dynamic range of the SAA3 measurements was limited as compared to the dynamic range of the neutrophil influx. The linear regression analysis of predictors of plasma SAA3 only identified physicochemical predictors, which were also predictors of neutrophil influx. We identified fewer predictors for SAA3 than for neutrophil influx, suggesting that neutrophil influx is a more sensitive and robust biomarker of inflammation and acute phase response in mice than plasma SAA3. As neutrophil is a robust biomarker and available in most inhalation studies on nanomaterials, this appears as an attractive proxy for CNT-induced SAA3 levels in mice with no difference between MWCNTs and SWCNTs.

It is well-established that long, needle-like MWCNTs represented by MWNT-7 are carcinogenic (Kasai et al., 2016). On the other hand, in the present analyses, all the different proxies for deposited surface area (BET, diameter and multi) predicted inflammation and less consistently acute phase response. This suggests that inflammation and acute phase response as important key events are especially induced by thin CNTs, since these have high specific surface area. Inflammation is an early key event in adverse outcome pathways leading to fibrosis and cardiovascular disease, and also cancer (Halappanavar et al., 2020; 2021). In agreement with this, two sub-chronic inhalation studies in rats with short and thin CNTs and long post-exposure follow-up have reported long-lasting pulmonary inflammation, and to a lesser extend fibrosis (Pauluhn, 2010, Pothmann et al., 2015), and pulmonary dosing of thin and entangled CNTs also induced adenocarcinomas in rats (Saleh et al., 2021; Saleh et al., 2022).

5. Conclusions

Pulmonary inflammation in terms of neutrophil influx and acute phase response in terms of SAA3 protein in plasma were equally induced by SWCNTs and MWCNTs in the present study. The SAA3 protein levels correlated closely with neutrophil influx across CNT types and post-exposure time points suggesting that SAA blood levels and neutrophil influx can be used as proxies for each other. By combining previous datasets of CNTs, we obtain large gradients in various physicochemical properties. However, we still observe co-variation and were therefore unable to separate effects of important properties such as BET surface area and length in the multiple regression analyses. Importantly, dose was consistently identified as an important predictor of inflammation and acute phase response. The cluster which included BET as the best proxy was also identified as an important predictor when SWCNT were analyzed separately. Mn and Fe were shown to be predictive for a higher neutrophil influx at day 1 after exposure, whereas the Ni content was associated with lower neutrophil influx response at all three time points and of lowered acute phase response at day 1 and 3 months.

Funding

This work was supported by the Danish Centre for Nanosafety, grant # 20110092173-3 from the Danish Working Environment Research Foundation, The Danish Centre for Nanosafety II, the European Union Seventh Framework Programme (FP7/2007-2013) under grant agreement no 310584 NANoREG, FFIKA, Focused Research Effort on Chemicals in the Working Environment from the Danish Government, the European Union's Horizon 2020 research and innovation programme under grant agreement 953183 HARMLESS.

CRediT authorship contribution statement

Per Axel Clausen: Writing – review & editing, Investigation, Formal analysis. **Kristina Bram Knudsen:** Writing – review & editing, Investigation, Formal analysis, Conceptualization. **Sarah Søs Poulsen:** Writing – review & editing, Visualization, Investigation, Formal analysis. **Pernille Høgh Danielsen:** Writing – review & editing, Writing – original draft, Visualization, Investigation, Formal analysis. **Ulla Vogel:** Writing – review & editing, Writing – original draft, Visualization, Funding acquisition, Formal analysis. **Håkan Wallin:** Writing – review & editing, Conceptualization. **Keld Alstrup Jensen:** Writing – review & editing, Investigation, Formal analysis.

Declaration of Competing Interest

The authors declare that they have no known competing financial interests or personal relationships that could have appeared to influence the work reported in this paper.

Data Availability

Data will be made available on reasonable request.

Acknowledgements

The excellent technical assistance from Michael Guldbrandsen, Eva Terrida, Lourdes Pedersen, Elzbieta Christiansen, Anne-Karin Asp, Zdenka Orabi Kyjovska, and Noor Irmam is greatly appreciated.

Appendix A. Supporting information

Supplementary data associated with this article can be found in the online version at doi:10.1016/j.etap.2024.104413.

References

Bengtson, S., Knudsen, K.B., Kyjovska, Z.O., et al., 2017. Differences in inflammation and acute phase response but similar genotoxicity in mice following pulmonary exposure to graphene oxide and reduced graphene oxide. PLoS One 12 (6), e0178355. https://doi.org/10.1371/journal.pone.0178355.

Bergamaschi, E., Garzaro, G., Jones, G.W., et al., 2021. Occupational exposure to carbon nanotubes and carbon nanofibres: more than a cobweb. Nanomaterials 11 (3), 745. https://doi.org/10.3390/nano11030745.

Bornholdt, J., Saber, A.T., Lilje, B., et al., 2017. Identification of gene transcription start sites and enhancers responding to pulmonary carbon nanotube exposure in vivo. ACS Nano 11 (4), 3597–3613. https://doi.org/10.1021/acsnano.6b07533.

Bredow, S., Falgout, M.M., March, T.H., et al., 2007. Subchronic inhalation of soluble manganese induces expression of hypoxia-associated angiogenic genes in adult mouse lungs. Toxicol. Appl. Pharmacol. 221 (2), 148–157. https://doi.org/10.1016/j.taap.2007.03.010.

Canu, I.G., Batsungnoen, K., Maynard, A., Hopf, N.B., 2020. State of knowledge on the occupational exposure to carbon nanotubes. Int J. Hyg. Environ Heal. 225 https://doi.org/10.1016/j.ijheh.2020.113472.

Christophersen, D.V., Moller, P., Thomsen, M.B., et al., 2021. Accelerated atherosclerosis caused by serum amyloid A response in lungs of ApoE(-/-) mice. FASEB J. 35 (3), e21307 https://doi.org/10.1096/fj.202002017R.

Cosnier, F., Seidel, C., Valentino, S., et al., 2021. Retained particle surface area dose drives inflammation in rat lungs following acute, subacute, and subchronic inhalation of nanomaterials. Part Fibre Toxicol. 18 (1), 29. https://doi.org/10.1186/s12989-021-00419-w.

Danielsen, P.H., Knudsen, K.B., Strancar, J., et al., 2020. Effects of physicochemical properties of TiO2 nanomaterials for pulmonary inflammation, acute phase response and alveolar proteinosis in intratracheally exposed mice. Toxicol. Appl. Pharmacol. 386, 114830 https://doi.org/10.1016/j.taap.2019.114830.

De Volder, M.F., Tawfick, S.H., Baughman, R.H., Hart, A.J., 2013. Carbon nanotubes: present and future commercial applications. Science 339 (6119), 535–539. https://doi.org/10.1126/science.1222453.

Di Ianni, E., Moller, P., Mortensen, A., et al., 2020. Organomodified nanoclays induce less inflammation, acute phase response, and genotoxicity than pristine nanoclays in mice lungs. Nanotoxicology 14 (7), 869–892. https://doi.org/10.1080/17435390.2020.1771786.

Dong, J., Ma, Q., 2019. Integration of inflammation, fibrosis, and cancer induced by carbon nanotubes. Nanotoxicology 13 (9), 1244–1274. https://doi.org/10.1080/17435390.2019.1651920.

Dong, Z., Wu, T., Qin, W., et al., 2011. Serum amyloid A directly accelerates the progression of atherosclerosis in apolipoprotein E-deficient mice. Mol. Med. 17 (11-12), 1357–1364. https://doi.org/10.2119/molmed.2011.00186.

Fraser, K., Hubbs, A., Yanamala, N., 2021. Histopathology of the broad class of carbon nanotubes and nanofibers used or produced in U.S. facilities in a murine model. Part Fibre Toxicol. 18 (1), 47. https://doi.org/10.1186/s12989-021-00440-z.

Gabay, C., Kushner, I., 1999. Acute-phase proteins and other systemic responses to inflammation. New Engl. J. Med. 340 (6), 448–454. https://doi.org/10.1056/NEJM199902113400607.

Gandhi, D., Rudrashetti, A.P., Rajasekaran, S., 2022. The impact of environmental and occupational exposures of manganese on pulmonary, hepatic, and renal functions. J. Appl. Toxicol. 42 (1), 103–129. https://doi.org/10.1002/jat.4214.

Gate, L., Knudsen, K.B., Seidel, C., et al., 2019. Pulmonary toxicity of two different multi-walled carbon nanotubes in rat: Comparison between intratracheal instillation and inhalation exposure. Toxicol. Appl. Pharmacol. 375, 17–31. https://doi.org/10.1016/j.taap.2019.05.001.

Gelli, K., Porika, M., Anreddy, R.N., 2015. Assessment of pulmonary toxicity of MgO nanoparticles in rats. Environ. Toxicol. 30 (3), 308–314. https://doi.org/10.1002/tox.21908.

Gutierrez, C.T., Loizides, C., Hafez, I., et al., 2023. Acute phase response following pulmonary exposure to soluble and insoluble metal oxide nanomaterials in mice. Part Fibre Toxicol. 20 (1), 4. https://doi.org/10.1186/s12989-023-00514-0.

Hadrup, N., Bengtson, S., Jacobsen, N.R., et al., 2017. Influence of dispersion medium on nanomaterial-induced pulmonary inflammation and DNA strand breaks: investigation of carbon black, carbon nanotubes and three titanium dioxide nanoparticles. Mutagenesis 32, 581–597. https://doi.org/10.1093/mutage/gex042.

Hadrup, N., Rahmani, F., Jacobsen, N.R., et al., 2019. Acute phase response and inflammation following pulmonary exposure to low doses of zinc oxide nanoparticles in mice. Nanotoxicology 13 (9), 1275–1292. https://doi.org/10.1080/17435390.2019.1654004.

Hadrup, N., Zhernovkov, V., Jacobsen, N.R., et al., 2020. Acute Phase Response as a Biological Mechanism-of-Action of (Nano)particle-Induced Cardiovascular Disease. Small 16 (21), e1907476. https://doi.org/10.1002/smll.201907476.

Hadrup, N., Aimonen, K., Ilves, M., et al., 2021. Pulmonary toxicity of synthetic amorphous silica - effects of porosity and copper oxide doping. Nanotoxicology 5 (1), 96–113. https://doi.org/10.1080/17435390.2020.1842932.

Halappanavar, S., van den Brule, S., Nymark, P., et al., 2020. Adverse outcome pathways as a tool for the design of testing strategies to support the safety assessment of emerging advanced materials at the nanoscale. Part Fibre Toxicol. 17 (1), 16. https://doi.org/10.1186/s12989-020-00344-4.

Halappanavar, S., Ede, J.D., Mahapatra, I., et al., 2021a. A methodology for developing key events to advance nanomaterial-relevant adverse outcome pathways to inform risk assessment. Nanotoxicology 15 (3), 289–310. https://doi.org/10.1080/17435390.2020.1851419.

Halappanavar, S., Nymark, P., Krug, H.F., Clift, M.J.D., Rothen-Rutishauser, B., Vogel, U., 2021b. Non-Animal Strategies for Toxicity Assessment of Nanoscale Materials: Role of Adverse Outcome Pathways in the Selection of Endpoints. Small 17 (15), e2007628. https://doi.org/10.1002/smll.202007628.

Halappanavar S., Sharma M., Solorio-Rodriguez S., et al. (2023). Substance interaction with the pulmonary resident cell membrane components leading to pulmonary fibrosis, OECD Series on Adverse Outcome Pathways, No. 33, OECD Publishing, Paris, doi:10.1787/10372cb8-en.

IARC (2017). Some Nanomaterials and Some Fibres IARC Monographs on the Evaluation of Carcinogenic Risks to Humans, No 111. IARC Monographs on the Evaluation of Carcinogenic Risks to Humans, Lyon (FR).

Jackson, P., Kling, K., Jensen, K.A., et al., 2015. Characterization of genotoxic response to 15 multiwalled carbon nanotubes with variable physicochemical properties including surface functionalizations in the FE1-Muta(TM) mouse lung epithelial cell line. Environ. Mol. Mutagen. 56 (2), 183–203. https://doi.org/10.1002/em.21922.

Jensen, K.A., Bøgelund, J., Jackson, P., et al., 2015. Carbon nanotubes - Types, products, market, and provisional assessment of the associated risks to man and the environment. Environ. Proj. 1805 (No), 2015 https://www2.mst.dk/Udgiv/publications/2015/12/978-87-93352-98-8.pdf.

Kasai, T., Umeda, Y., Ohnishi, M., et al., 2015. Thirteen-week study of toxicity of fiber-like multi-walled carbon nanotubes with whole-body inhalation exposure in rats. Nanotoxicology 9 (4), 413–422. https://doi.org/10.3109/17435390.2014.933903.

Kasai, T., Umeda, Y., Ohnishi, M., et al., 2016. Lung carcinogenicity of inhaled multi-walled carbon nanotube in rats. Part Fibre Toxicol. 13 (1), 53. https://doi.org/10.1186/s12989-016-0164-2.

King, V.L., Thompson, J., Tannock, L.R., 2011. Serum amyloid A in atherosclerosis. Curr. Opin. Lipido 22 (4), 302–307. https://doi.org/10.1097/MOL.0b013e3283488c39.

Knudsen, K.B., Berthing, T., Jackson, P., et al., 2019. Physicochemical predictors of Multi-Walled Carbon Nanotube-induced pulmonary histopathology and toxicity one year after pulmonary deposition of 11 different Multi-Walled Carbon Nanotubes in mice. Basic Clin. Pharm. Toxicol. 124 (2), 211–227. https://doi.org/10.1111/bcpt.13119.

Labib, S., Williams, A., Yauk, C.L., et al., 2016. Nano-risk Science: application of toxicogenomics in an adverse outcome pathway framework for risk assessment of multi-walled carbon nanotubes. Part Fibre Toxicol. 13, 15. https://doi.org/10.1186/s12989-016-0125-9.

Lee, S., Hwang, S.H., Jeong, J., et al., 2016. Nickel oxide nanoparticles can recruit eosinophils in the lungs of rats by the direct release of intracellular eotaxin. Part Fibre Toxicol. 13 (1), 30. https://doi.org/10.1186/s12989-016-0142-8.

Ma-Hock, L., Treumann, S., Strauss, V., et al., 2009. Inhalation toxicity of multiwall carbon nanotubes in rats exposed for 3 months. Toxicol. Sci. 112 (2), 468–481. https://doi.org/10.1093/toxsci/kfp146.

Monsé, C., Hagemeyer, O., Raulf, M., et al., 2018. Concentration-dependent systemic response after inhalation of nano-sized zinc oxide particles in human volunteers. Part Fibre Toxicol. 15 (1), 8. https://doi.org/10.1186/s12989-018-0246-4.

Murphy, F., Dekkers, S., Braakhuis, H., et al., 2021. An integrated approach to testing and assessment of high aspect ratio nanomaterials and its application for grouping based on a common mesothelioma hazard. NanoImpact 22, 100314. https://doi.org/10.1016/j.impact.2021.100314.

Murphy, F., Jacobsen, N.R., Di Ianni, E., et al., 2022. Grouping MWCNTs based on their similar potential to cause pulmonary hazard after inhalation: a case-study. Part Fibre Toxicol. 19 (1), 50. https://doi.org/10.1186/s12989-022-00487-6.

Nikota, J., Williams, A., Yauk, C.L., Wallin, H., Vogel, U., Halappanavar, S., 2016. Meta-analysis of transcriptomic responses as a means to identify pulmonary disease outcomes for engineered nanomaterials. Part Fibre Toxicol. 13 (1), 25. https://doi.org/10.1186/s12989-016-0137-5.

Nikota, J., Banville, A., Goodwin, L.R., et al., 2017. Stat-6 signaling pathway and not Interleukin-1 mediates multi-walled carbon nanotube-induced lung fibrosis in mice: insights from an adverse outcome pathway framework. Part Fibre Toxicol. 14 (1), 37. https://doi.org/10.1186/s12989-017-0218-0.

NIOSH (2013). Current intelligence bulletin 65: occupational exposure to carbon nanotubes and nanofibers. Cincinnati, OH: U.S. Department of Health and Human Services, Centers for Disease Control, National Institute for Occupational Safety and Health, DHHS (NIOSH) Publication No. 2013–145.

Nymark, P., Karlsson, H.L., Halappanavar, S., Vogel, U., 2021. Adverse Outcome Pathway Development for Assessment of Lung Carcinogenicity by Nanoparticles. Front Toxicol. 3, 653386 https://doi.org/10.3389/ftox.2021.653386.

Pauluhn, J., 2010. Subchronic 13-week inhalation exposure of rats to multiwalled carbon nanotubes: toxic effects are determined by density of agglomerate structures, not fibrillar structures. Toxicol. Sci. 113 (1), 226–242. https://doi.org/10.1093/toxsci/kfp247.

Pothmann, D., Simar, S., Schuler, D., et al., 2015. Lung inflammation and lack of genotoxicity in the comet and micronucleus assays of industrial multiwalled carbon nanotubes Graphistrength(©) C100 after a 90-day nose-only inhalation exposure of rats. Part Fibre Toxicol. 12, 21. https://doi.org/10.1186/s12989-015-0096-2.

Poulsen, S.S., Jackson, P., Kling, K., et al., 2016. Multi-walled carbon nanotube physicochemical properties predict pulmonary inflammation and genotoxicity. Nanotoxicology 10 (9), 1263–1275. https://doi.org/10.1080/17435390.2016.1202351.

Poulsen, S.S., Knudsen, K.B., Jackson, P., et al., 2017. Multi-walled carbon nanotube-physicochemical properties predict the systemic acute phase response following pulmonary exposure in mice. PLoS One 12 (4), e0174167. https://doi.org/10.1371/journal.pone.0174167.

Poulsen, S.S., Saber, A.T., Williams, A., et al., 2015a. MWCNTs of different physicochemical properties cause similar inflammatory responses, but differences in transcriptional and histological markers of fibrosis in mouse lungs. Toxicol. Appl. Pharmacol. 284 (1), 16–32. https://doi.org/10.1016/j.taap.2014.12.011.

Poulsen, S.S., Saber, A.T., Mortensen, A., et al., 2015b. Changes in cholesterol homeostasis and acute phase response link pulmonary exposure to multi-walled carbon nanotubes to risk of cardiovascular disease. Toxicol. Appl. Pharm. 283 (3), 210–222. https://doi.org/10.1016/j.taap.2015.01.011.

Poulsen, S.S., Jacobsen, N.R., Labib, S., et al., 2013. Transcriptomic analysis reveals novel mechanistic insight into murine biological responses to multi-walled carbon nanotubes in lungs and cultured lung epithelial cells. PLoS One 8 (11), e80452. https://doi.org/10.1371/journal.pone.0080452.

RAC (2022). The Committee for Risk Assessment. Opinion proposing harmonised classification and labelling at EU level of Multi-Walled Carbon Tubes (synthetic graphite in tubular shape) with a geometric tube diameter range $\geq$ 30 nm to $<$ 3 µm and a length $\geq$ 5 µm and aspect ratio $\geq$ 3:1, including Multi-Walled Carbon Nanotubes, MWC(N)T.

Rahman, L., Jacobsen, N.R., Aziz, S.A., et al., 2017. Multi-walled carbon nanotube-induced genotoxic, inflammatory and pro-fibrotic responses in mice: Investigating the mechanisms of pulmonary carcinogenesis. Mutat. Res. Genet. Toxicol. Environ. Mutagen. 823, 28–44. https://doi.org/10.1016/j.mrgentox.2017.08.005.

Rittinghausen, S., Hackbarth, A., Creutzenberg, O., et al., 2014. The carcinogenic effect of various multi-walled carbon nanotubes (MWCNTs) after intraperitoneal injection in rats. Part Fibre Toxicol. 11, 59. https://doi.org/10.1186/s12989-014-0059-z.

Roach, K.A., Stefaniak, A.B., Roberts, J.R., 2019. Metal nanomaterials: Immune effects and implications of physicochemical properties on sensitization, elicitation, and exacerbation of allergic disease. J. Immunotoxicol. 16 (1), 87–124. https://doi.org/10.1080/1547691X.2019.1605553.

Saber, A.T., Jacobsen, N.R., Mortensen, A., et al., 2012. Nanotitanium dioxide toxicity in mouse lung is reduced in sanding dust from paint. Part Fibre Toxicol. 9, 4. https://doi.org/10.1186/1743-8977-9-4.

Saber, A.T., Lamson, J.S., Jacobsen, N.R., et al., 2013. Particle-induced pulmonary acute phase response correlates with neutrophil influx linking inhaled particles and cardiovascular risk. PLoS One 8 (7), e69020. https://doi.org/10.1371/journal.pone.0069020.

Saber, A.T., Jacobsen, N.R., Jackson, P., et al., 2014. Particle-induced pulmonary acute phase response may be the causal link between particle inhalation and cardiovascular disease. Wiley Inter. Rev. Nanomed. Nanobiotechnol. 6 (6), 517–531. https://doi.org/10.1002/wnan.1279.

Saber, A.T., Mortensen, A., Szarek, J., et al., 2016. Epoxy composite dusts with and without carbon nanotubes cause similar pulmonary responses, but differences in liver histology in mice following pulmonary deposition. Part Fibre Toxicol. 13 (1), 37. https://doi.org/10.1186/s12989-016-0148-2.

Saleh, D.M., Alexander, W.T., Numano, T., et al., 2021. Comparative carcinogenicity study of a thick, straight-type and a thin, tangled-type multi-walled carbon nanotube administered by intra-tracheal instillation in the rat. Part Fibre Toxicol. 17 (1), 48. https://doi.org/10.1186/s12989-020-00382-y.

Saleh, D.M., Luo, S., Ahmed, O.H.M., et al., 2022. Assessment of the toxicity and carcinogenicity of double-walled carbon nanotubes in the rat lung after intratracheal instillation: a two-year study. Part Fibre Toxicol. 19 (1), 30. https://doi.org/10.1186/s12989-022-00469-8.

Serra, A., Del Giudice, G., Kinaret, P.A.S., et al., 2022. Characterization of ENM dynamic dose-dependent MOA in lung with respect to immune cells infiltration. Nanomaterials (Basel) 12 (12). https://doi.org/10.3390/nano12122031.

Solorio-Rodriguez, S.A., Williams, A., Poulsen, S.S., et al., 2023. Single-Walled vs. Multi-Walled Carbon Nanotubes: Influence of Physico-Chemical Properties on Toxicogenomics Responses in Mouse Lungs. Nanomaterials 13 (6). https://doi.org/10.3390/nano13061059.

Thompson, J.C., Wilson, P.G., Shridas, P., et al., 2018. Serum amyloid A3 is pro-atherogenic. Atherosclerosis 268, 32–35. https://doi.org/10.1016/j.atherosclerosis.2017.11.011.